

## Article

# New Dinitrophenyl Hydrazones as Colorimetric Probes for Anions

Rui P. C. L. Sousa <sup>†</sup>, Susana P. G. Costa <sup>†</sup>, Rita B. Figueira <sup>\*</sup> and M. Manuela M. Raposo <sup>\*</sup>

Centre of Chemistry, University of Minho, Campus de Gualtar, 4710-057 Braga, Portugal

<sup>\*</sup> Correspondence: rbacelarfigueira@quimica.uminho.pt (R.B.F.); mfox@quimica.uminho.pt (M.M.M.R.)<sup>†</sup> These authors contributed equally to this work.

**Abstract:** Anion sensing is a dynamic research field due to the biological and environmental importance of some organic or inorganic anions. Hydrazones show promising properties in the design of anion chemosensors due to the presence of proton donor and acceptor sites in their structure. In this work, two novel dinitrophenyl hydrazones, functionalized with a quinoline moiety, were synthesized and characterized by spectroscopic and spectrometric techniques. The interaction between the new compounds **3a–b** with different organic and inorganic anions was assessed. The two compounds showed a change in color from light yellow to magenta in the presence of  $\text{H}_2\text{PO}_4^-$ ,  $\text{CH}_3\text{COO}^-$ ,  $\text{BzO}^-$ ,  $\text{CN}^-$ , and  $\text{F}^-$ . The interactions were analyzed by spectrophotometric titrations and the stoichiometry of the interaction was assessed by the method of continuous variation. Compound **3b** showed a remarkable sensitivity to  $\text{CN}^-$ , with a limit of detection of  $0.35 \mu\text{M}$ . The interaction of compound **3b** with  $\text{CN}^-$  and  $\text{F}^-$  was also analyzed by  $^1\text{H}$  NMR titrations, showing that an increasing concentration of anions induce a deprotonation of the NH and OH groups.

**Keywords:** anions; colorimetric chemosensor; hydrazone; synthesis; quinoline



**Citation:** Sousa, R.P.C.L.; Costa, S.P.G.; Figueira, R.B.; Raposo, M.M.M. New Dinitrophenyl Hydrazones as Colorimetric Probes for Anions. *Chemosensors* **2022**, *10*, 384. <https://doi.org/10.3390/chemosensors10100384>

Academic Editor: Vardan Galstyan

Received: 22 August 2022

Accepted: 20 September 2022

Published: 23 September 2022

**Publisher's Note:** MDPI stays neutral with regard to jurisdictional claims in published maps and institutional affiliations.



**Copyright:** © 2022 by the authors. Licensee MDPI, Basel, Switzerland. This article is an open access article distributed under the terms and conditions of the Creative Commons Attribution (CC BY) license (<https://creativecommons.org/licenses/by/4.0/>).

## 1. Introduction

Colorimetric optical sensing is a desirable feature in the chemosensing field. Colorimetric optical sensors are used worldwide in simple and well-known devices such as pregnancy or glucose tests [1,2]. This class of sensors show some upper advantages compared to other sensor types, such as low-cost and selectivity [3]. Even though the sensibility is not as high as in fluorimetric sensors, they show a major benefit: the possibility of “naked eye” detection [3,4].

With the large number of available chromophores together with the simple methodology required, this type of sensing is attractive to develop straightforward methods for fast and simple detection of several analytes [5,6]. While most of the detection methods require sampling and laboratory analysis, which can be expensive and time consuming, a colorimetric chemosensor allows easy, on-site detection [7,8]. The design of organic chemosensors containing binding sites capable of sensing anions and cations is an interesting and promising field within the chemosensing area.

Anion sensing is particularly important due to the role that some anions (such as fluoride or cyanide) can have on biological and environmental systems [8–14]. For instance, cyanide is acutely toxic to mammals by all routes of administration, affecting cardiovascular, respiratory, and central nervous systems [14]. This anion's toxicity from smoke inhalation and the potential use of cyanide as a weapon of terrorism turn this analyte into one of the most relevant targets [14]. The European Union has a limit of  $50 \mu\text{g L}^{-1}$  for cyanide in drinking waters, and the maximum concentration allowed in mineral waters is  $70 \mu\text{g L}^{-1}$  [14].

Anions are generally challenging targets due to the wide range of sizes and shapes they can have [15,16]. The design of a chemosensor for anion sensing usually involves a binding site capable of establish several non-covalent interactions, such as hydrogen

bonding, electrostatic interactions, metal coordination, halogen bonding, and anion- $\pi$  interactions [17,18].

Schiff bases are particularly known for their interesting chemosensing properties [5,8,19]. Aryl-substituted Schiff bases are more stable and easier to synthesize due to their effective conjugation compared to alkyl-substituted Schiff bases [8,20]. Within this group, hydrazones are considered as both proton-donor and proton-acceptor moieties, which are promising structural characteristics in the design of chemosensors [21–27]. Besides, the C=N–N triatomic structure has nucleophilic imine and amino-type (more reactive) nitrogens, an imine carbon that has both an electrophilic and nucleophilic character, configurational isomerism stemming from the intrinsic nature of the C=N double bond, and, in most cases, an acidic NH [28]. The latter property is crucial in basic anion sensing.

The combination of the sensing characteristics of hydrazones with conjugated heterocyclic groups can be important in the development of an anion colorimetric sensor. The distance between HOMO and LUMO establishes the maximum absorption wavelength of the molecule, and the more conjugated the molecule, the lower the gap is between these two orbitals and the longer is the wavelength [4]. Quinoline is a type of heterocycle that can serve to functionalize hydrazones, in order to add electron density to the molecule and an extra heteroatom (nitrogen), which can be involved in the interaction with the analytes.

This work reports the synthesis of two new dinitrophenyl hydrazones, based on a quinoline moiety. The synthesized compounds were characterized by the usual spectroscopic and spectrometric techniques. The interaction in an acetonitrile (ACN) solution between the two novel compounds and several anions was tested. Spectrophotometric titrations were performed to assess the extension of the interaction. NMR titrations were also conducted to assess the binding site of the molecules involved in the interaction. One of the compounds synthesized showed a remarkable sensitivity to  $\text{CN}^-$ , with a limit of detection (LOD) of 0.35  $\mu\text{M}$ . This value is below the European Union limit, both for drinking and mineral waters, namely, 1.92 and 2.69  $\mu\text{M}$ , respectively. The two compounds synthesized are also sensitive to other anions, with LODs in the range of  $\mu\text{M}$ , based on its basicity. The sensitivity obtained is higher for  $\text{CN}^-$ , the most basic anion of the group of tested anions.

## 2. Experimental Section

### 2.1. Materials

Melting points were measured on a Stuart SMP3 melting-point apparatus. TLC analysis was carried out on 0.20 mm-thick precoated silica plates (Macherey-Nagel), and spots were observed under UV light on a CN-15 camera (Vilber Lourmat). Infrared spectra were obtained on a PerkinElmer Spectrum Two instrument with ATR accessory, in the 450–4000  $\text{cm}^{-1}$  range with 32 scans. The solid compound was applied directly on the ATR crystal, with pressure applied with the incorporated press. UV-Vis absorption spectra (200–700 nm) were obtained using a Shimadzu UV/3101PC spectrophotometer and fluorescence spectra with a Fluoromax-4 spectrofluorometer. NMR spectra were obtained on a Bruker Avance III 400 at an operating frequency of 400 MHz for  $^1\text{H}$  and 100.6 MHz for  $^{13}\text{C}$ , using the solvent peak as internal reference, at 25 °C. All chemical shifts are given in ppm, using  $\delta_{\text{H}} \text{Me}_4\text{Si} = 0$  ppm as the reference, and  $J$  values are given in Hz. Assignments were supported by spin decoupling–double resonance and bidimensional heteronuclear correlation techniques. All commercial reagents and solvents were used as received.

### 2.2. General Procedure for the Synthesis of Heterocyclic Quinoline-Based Hydrazones

Equal amounts (0.318 mmol) of the hydrazine and the appropriate aldehyde were dissolved in 10 mL of MeOH at room temperature. The reaction mixture was stirred for 8–10 h. The precipitated solid was filtered and dried in the oven at 40 °C overnight. No additional purification was required.

### 2.2.1. 2-((2-(2,4-Dinitrophenyl)hydrazineylidene)methyl)quinoline **3a**

Yellow solid (88%). Mp: 251 °C.  $^1\text{H}$  NMR (DMSO- $d_6$ , 400 MHz):  $\delta$  = 7.63 (dt,  $J$  = 7.6 and 1.2 Hz, 1H, H6'), 7.79 (dt,  $J$  = 7.6 and 1.2 Hz, 1H, H7'), 7.99 (dd,  $J$  = 8.0 and 1.2 Hz, 1H, H5'), 8.04 (dd,  $J$  = 8.4 and 0.4 Hz, 1H, H8'), 8.18–8.22 (m, 2H, H6 + H3'), 8.38–8.42 (m, 2H, H5 + H4'), 8.78 (s, 1H, N=CH), 8.86 (d,  $J$  = 2.4 Hz, 1H, H3), 11.76 (s, 1H, NH) ppm.  $^{13}\text{C}$  NMR (DMSO- $d_6$ , 100.6 MHz):  $\delta$  = 116.9 (C6), 117.5 (C3'), 122.3 (C3), 127.0 (C6'), 127.6 (C5'), 127.6 (C4a'), 128.7 (C8'), 129.2 (C5), 129.7 (C7'), 130.4 (C2), 136.3 (C4'), 137.8 (C4), 143.9 (C1), 147.2 (C8a'), 148.6 (N=CH), 153.0 (C2') ppm. IR (solid):  $\nu$  3278, 3169, 3107, 3007, 2147, 1969, 1944, 1836, 1619, 1613, 1584, 1546, 1522, 1503, 1460, 1431, 1375, 1337, 1322, 1309, 1280, 1270, 1244, 1223, 1144, 1096, 1058, 996, 962, 945, 916, 878, 859, 844, 834, 827, 791, 770, 759, 742, 714, 682, 637, 620, 599, 527, 513, 482  $\text{cm}^{-1}$ . HRMS: (ESI, positive mode)  $m/z$  for  $\text{C}_{16}\text{H}_{11}\text{N}_5\text{O}_4$ , calcd 336.0738; found 336.0746.

### 2.2.2. 2-((2-(2,4-Dinitrophenyl)hydrazineylidene)methyl)quinolin-8-ol **3b**

Yellow solid (95%). Mp: 298 °C.  $^1\text{H}$  NMR (DMSO- $d_6$ , 400 MHz):  $\delta$  = 7.14 (dd,  $J$  = 7.2 and 1.2 Hz, 1H, H7'), 7.45 (m, 2H, H5' + H6'), 8.23 (d,  $J$  = 8.8 Hz, 1H, H3'), 8.24 (d,  $J$  = 10 Hz, 1H, H6), 8.36 (d,  $J$  = 8.4 Hz, 1H, H4'), 8.41 (dd,  $J$  = 9.6 and 2.8 Hz, 1H, H5), 8.82 (s, 1H, N=CH), 8.87 (d,  $J$  = 2.8 Hz, 1H, H3), 9.89 (s, 1H, OH), 11.95 (s, 1H, NH) ppm.  $^{13}\text{C}$  NMR (DMSO- $d_6$ , 100.6 MHz):  $\delta$  = 112.3 (C7'), 117.3 (C6), 117.9 (C5'), 118.1 (C3'), 122.9 (C3), 128.6 (C6'), 128.9 (C4a'), 129.8 (C5), 130.5 (C2), 136.7 (C4'), 137.8 (C4), 138.3 (C8a'), 144.4 (C1), 148.4 (N=CH), 151.3 (C2'), 153.5 (C8') ppm. IR (solid):  $\nu$  3417, 3285, 3107, 2249, 2162, 1982, 1619, 1605, 1583, 1562, 1547, 1520, 1505, 1462, 1429, 1393, 1378, 1336, 1323, 1278, 1237, 1200, 1169, 1143, 1136, 1100, 1057, 1044, 975, 940, 925, 916, 883, 851, 834, 763, 741, 721, 714, 693, 684, 637, 590, 570, 535, 524, 507, 484, 461  $\text{cm}^{-1}$ . HRMS: (ESI, positive mode)  $m/z$  for  $\text{C}_{16}\text{H}_{11}\text{N}_5\text{O}_5$ , calcd 352.0687; found 352.0692.

## 2.3. Chemosensing Studies

In the preliminary studies, 50 equivalents (equiv.) of each ion (50  $\mu\text{L}$ ,  $1 \times 10^{-1}$  M in ACN) were added to an ACN solution of each compound (1 mL,  $1 \times 10^{-4}$  M). The assessment of the color/fluorescence changes was evaluated by “naked eye” and in a UV-vis chamber under ultraviolet light at 365 nm. All anions were in the form of hydrated tetrabutylammonium salts and solutions were prepared in UV-grade ACN. Spectrophotometric titrations were performed when a relevant optical response was observed. To an ACN solution of each compound (3 mL,  $1 \times 10^{-5}$  M), a sequential addition of each ion ( $10^{-2}$ – $10^{-3}$  M) was performed, and the absorbance spectra was collected, until the absorption plateau was reached. NMR titrations were performed by a similar sequential addition of each ion to a DMSO- $d_6$  solution of the compound. Job plots were obtained by the addition of different molar ratios of  $10^{-4}$  M solutions of the compounds and the corresponding ion. Limit of detection (LOD) and limit of quantification (LOQ) were calculated with the slope of the calibration curve, using 10 different analyses [29].

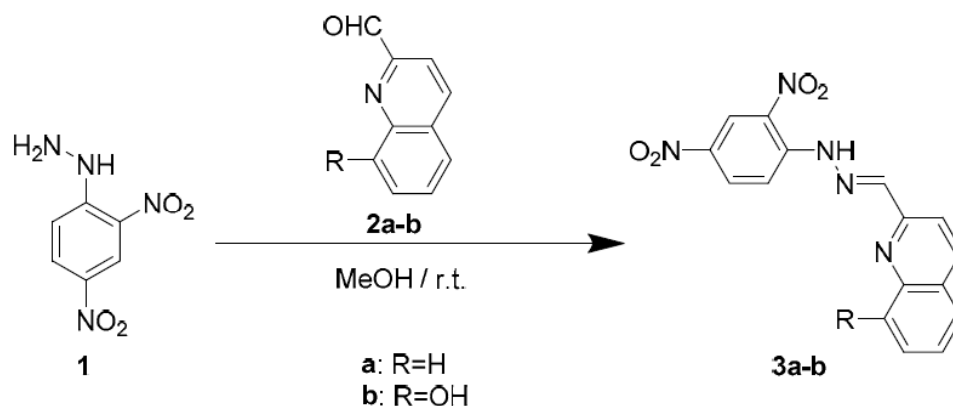
## 3. Results and Discussion

### 3.1. Synthesis of Heterocyclic Quinoline-Based Hydrazones

The new quinoline-based hydrazones **3a–b** were synthesized by reaction of (2,4-dinitrophenyl)hydrazine **1** with quinoline-2-carbaldehyde **2a** and 8-hydroxyquinoline-2-carbaldehyde **2b**, respectively, in methanol at room temperature for 8–10 h (*vide* Scheme 1). The resulting solids were then filtered, and the pure compounds were isolated with yields of 88% and 95%, respectively, and characterized by the usual spectroscopic techniques.

The  $^1\text{H}$  NMR spectra of compound **3b** shows the signal for hydrazone NH at 11.76 ppm, OH signal at 9.89 ppm, and the imine N=CH at 8.82 ppm. Besides, the protons from the quinoline moiety appear at 7.14 (H7'), 7.45 (H5' + H6'), 8.23 (H3'), and 8.36 (H4') ppm. Dinitrophenyl protons appear at higher chemical shifts, due to the deshielding effect caused by the  $\text{NO}_2$  groups: 8.24 (H6), 8.41 (H5), and 8.87 (H3) ppm. In the spectra of **3a**, the main difference is the presence of H8' at 8.04 ppm. The remaining quinoline protons appear at

7.63 (H6'), 7.79 (H7'), and 7.99 (H5') ppm. H3' and H4' appear in the multiplet signals together with H6 and H5 from the dinitrophenyl groups, at 8.18–8.22 and 8.38–8.42 ppm. The imine N=CH appears at 8.78 ppm, as well as hydrazone NH at 11.76, similarly to **3b**. <sup>13</sup>C RMN spectra of **3b** reveal a downfield shift of C8' (153.5 ppm), when compared with the spectra of **3a** (128.7 ppm), due to the presence of the -OH group. FTIR spectra of compound **3b** also shows the OH bending vibration at 1393 cm<sup>-1</sup>.



**Scheme 1.** Synthesis of the quinoline-based hydrazones **3a–b**.

The two compounds were dissolved in ACN ( $1 \times 10^{-5}$  M) for the photophysical characterization, resulting in a light-yellow solution in both cases. UV/Vis spectra of the two compounds are similar, with a maximum absorption wavelength ( $\lambda_{\text{abs}}$ ) of 379 nm for hydrazone **3a** and 385 for hydrazone **3b**. The logarithm of the molar attenuation coefficient ( $\log \epsilon$ ) values were found to be 4.51 and 4.46, respectively.

### 3.2. Preliminary Chemosensory Tests

Evaluation of the new 2,4-dinitrophenylhydrazones **3a–b**, as potential anion colorimetric/fluorimetric chemosensors, was carried out by performing preliminary sensory tests in ACN in the presence of analytically relevant organic and inorganic anions ( $\text{H}_2\text{PO}_4^-$ ,  $\text{CH}_3\text{COO}^-$ ,  $\text{NO}_3^-$ ,  $\text{ClO}_4^-$ ,  $\text{HSO}_4^-$ ,  $\text{BzO}^-$ ,  $\text{Br}^-$ ,  $\text{CN}^-$ ,  $\text{I}^-$ , and  $\text{F}^-$ ). Preliminary tests were carried out by addition of 50 equiv. of each ion to the solutions of compounds **3a–b**. For the two compounds, a change in color from light-yellow to magenta was visible upon interaction with several anions, namely,  $\text{H}_2\text{PO}_4^-$ ,  $\text{CH}_3\text{COO}^-$ ,  $\text{BzO}^-$ ,  $\text{CN}^-$ , and  $\text{F}^-$  (vide Figure 1). The two compounds were also tested with different cations, with no significant optical response.

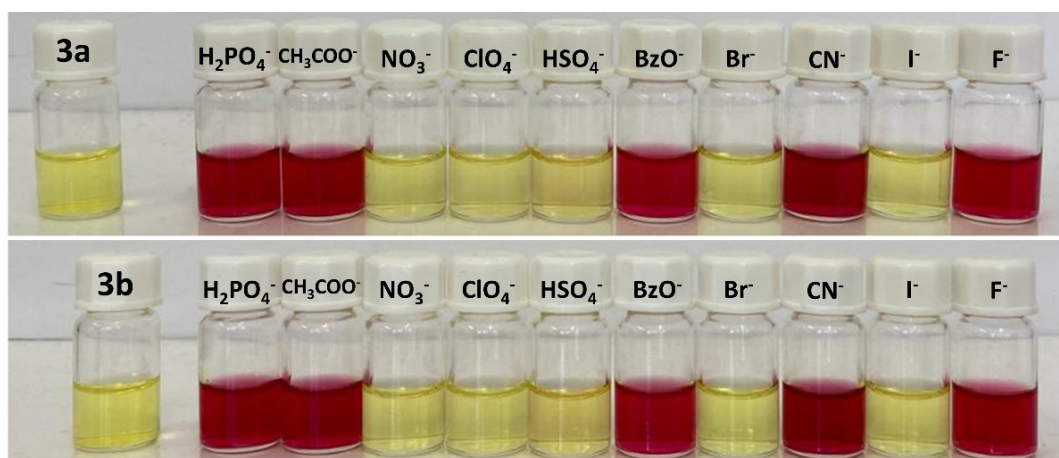


**Figure 1.** Preliminary chemosensory tests of compounds **3a–b** upon interaction with different anions.

### 3.3. Spectrophotometric Titrations

The interaction between the two compounds **3a–b** with the five anions ( $\text{H}_2\text{PO}_4^-$ ,  $\text{CH}_3\text{COO}^-$ ,  $\text{BzO}^-$ ,  $\text{CN}^-$ , and  $\text{F}^-$ ), which resulted in a color change, was analyzed by spectrophotometric titrations. To 3 mL of a  $10^{-5}$  M ACN solution of each compound, successive amounts of each anion were added until a plateau was reached. Figures 2–6 show the spectrophotometric titrations for compound **3b** (**3a** showed similar results), as well as the Job's plot for the determination of stoichiometry by the method of continuous variation.

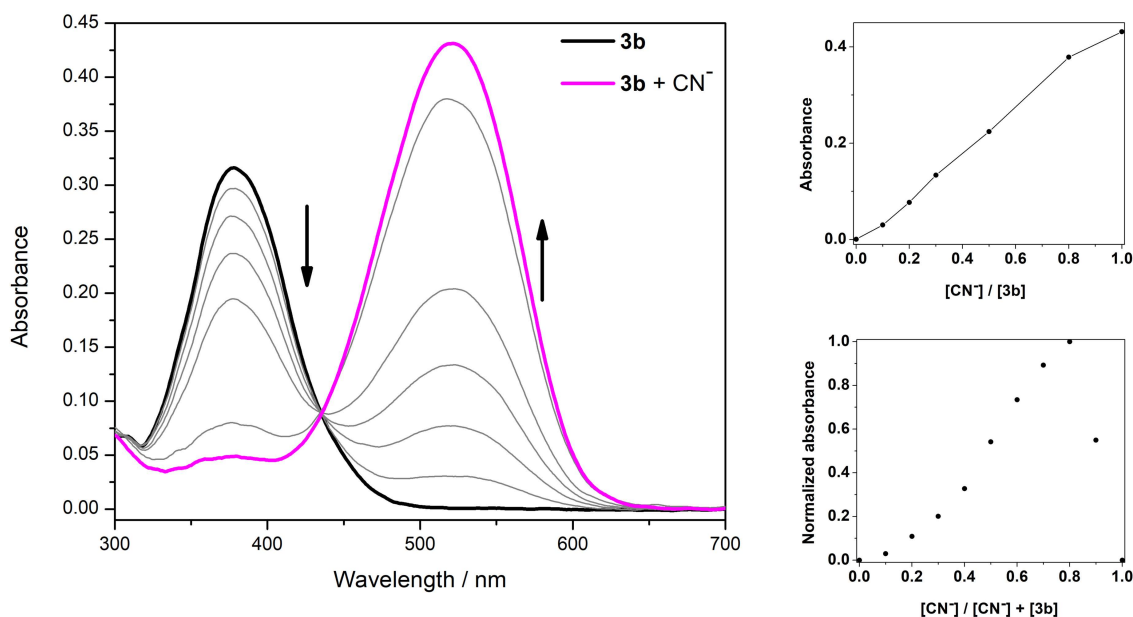


**Figure 2.** Photophysical interaction between compound **3b** and  $\text{CN}^-$  (1 equiv. of  $\text{CN}^-$  required for maximum absorbance). **Left**—spectrophotometric titration of compound **3b** with  $\text{CN}^-$ ; **Top right**—absorbance at 520 nm as a function of added ion equiv.; **Bottom right**—Job's plot for the interaction (stoichiometry **3b** 1:3  $\text{CN}^-$ ).

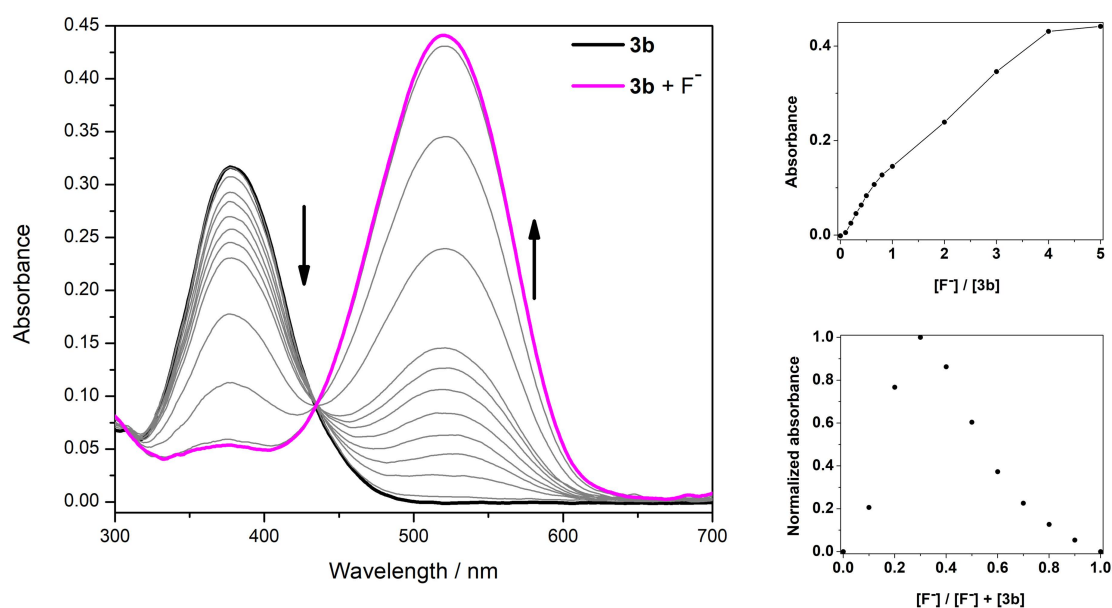


**Figure 3.** Photophysical interaction between compound **3b** and  $\text{F}^-$  (5 equiv. of  $\text{F}^-$  required for maximum absorbance). **Left**—spectrophotometric titration of compound **3b** with  $\text{F}^-$ ; **Top right**—absorbance at 520 nm as a function of added ion equiv.; **Bottom right**—Job's plot for the interaction (stoichiometry **3b** 2:1  $\text{F}^-$ ).

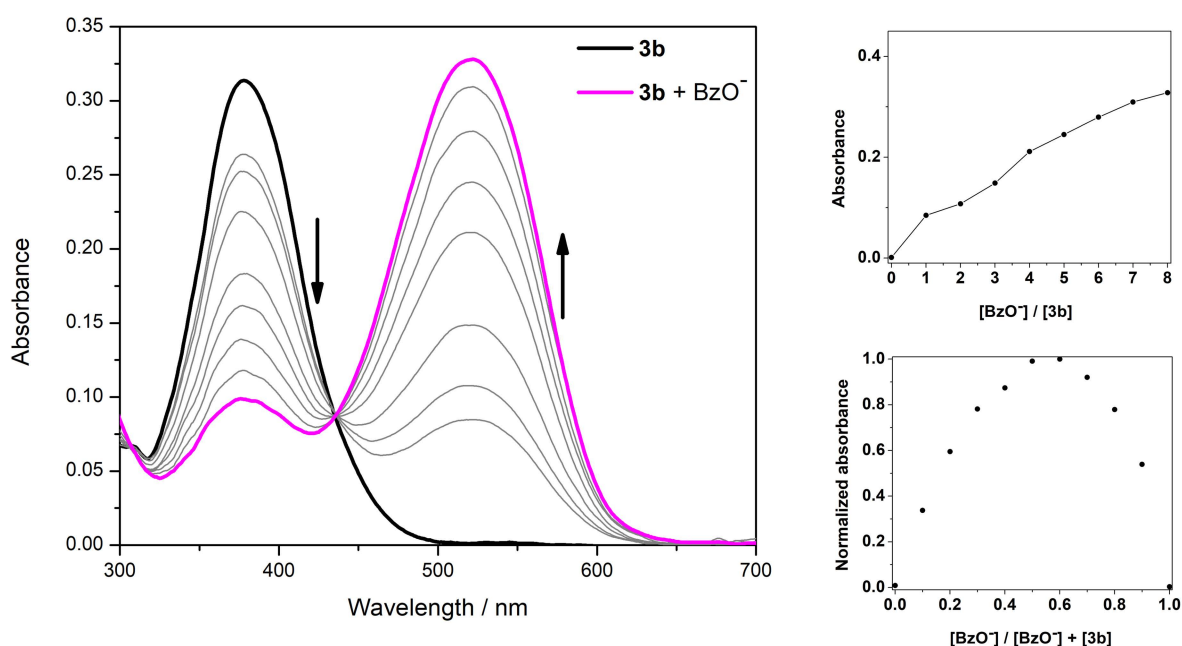


**Figure 4.** Photophysical interaction between compound **3b** and  $\text{BzO}^-$  (8 equiv. of  $\text{BzO}^-$  required for maximum absorbance). **Left**—spectrophotometric titration of compound **3b** with  $\text{BzO}^-$ ; **Top right**—absorbance at 520 nm as a function of added ion equiv.; **Bottom right**—Job's plot for the interaction (stoichiometry **3b** 1:1  $\text{BzO}^-$ ).

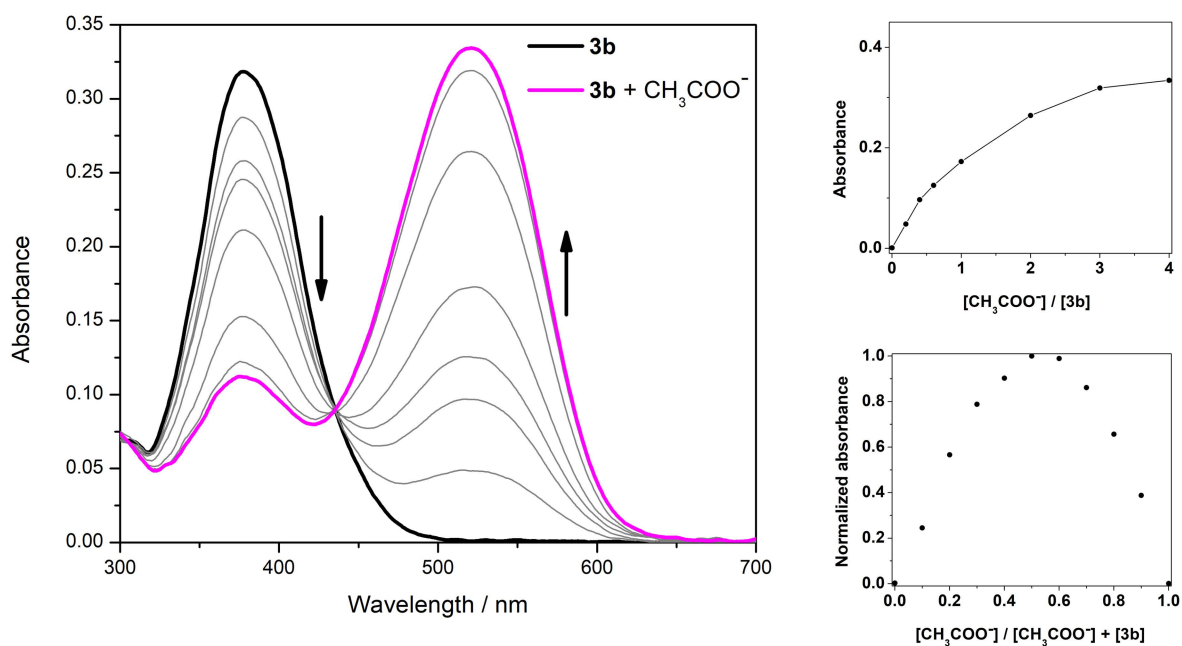


**Figure 5.** Photophysical interaction between compound **3b** and  $\text{CH}_3\text{COO}^-$  (4 equiv. of  $\text{CH}_3\text{COO}^-$  required for maximum absorbance). **Left**—spectrophotometric titration of compound **3b** with  $\text{CH}_3\text{COO}^-$ ; **Top right**—absorbance at 520 nm as a function of added ion equiv.; **Bottom right**—Job's plot for the interaction (stoichiometry **3b** 1:1  $\text{CH}_3\text{COO}^-$ ).

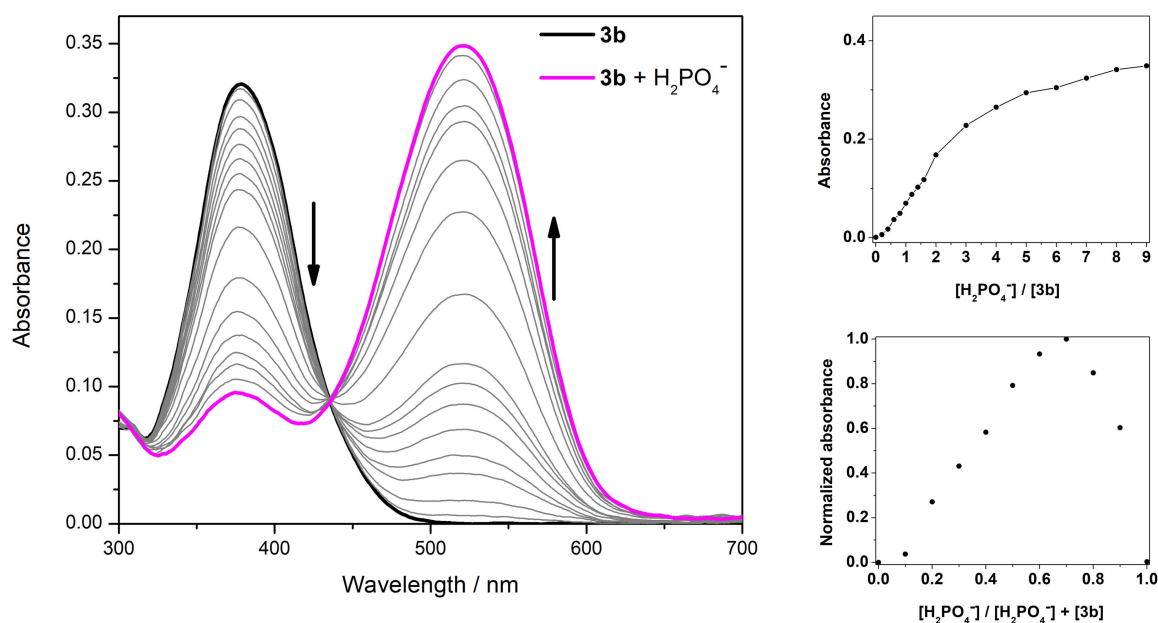


**Figure 6.** Photophysical interaction between compound **3b** and  $\text{H}_2\text{PO}_4^-$  (9 equiv. of  $\text{H}_2\text{PO}_4^-$  required for maximum absorbance). **Left**—spectrophotometric titration of compound **3b** with  $\text{H}_2\text{PO}_4^-$ ; **Top right**—absorbance at 520 nm as a function of added ion equiv.; **Bottom right**—Job's plot for the interaction (stoichiometry **3b** 1:2  $\text{H}_2\text{PO}_4^-$ ).

The behavior of compound **3b** in the presence of the five anions is similar. The main band in the visible zone (385 nm) reduces intensity upon sequential addition of each ion, while a new band at 520 nm is formed. Job's plots show the stoichiometry of each interaction, which changes from one anion to another, but is similar for compounds **3a–b**. The sensitivity of the hydrazones towards the five anions is high, being necessary between 1 to 10 equiv. of the anion to achieve the maximal optical change. It can be observed that compound **3b** showed higher sensitivity to  $\text{CN}^-$  and the interaction with  $\text{H}_2\text{PO}_4^-$  and  $\text{BzO}^-$  required a higher number of equiv. to reach the absorption plateau. The LOD and the LOQ for the interaction between the two hydrazones and the five anions were calculated through the slope of the linear zone of each absorbance *vs.* the number of equiv. graphs. The results are shown in Table 1.

**Table 1.** LOD and LOQ of compounds **3a–b** for the five anions in ACN.

|                       | Compound  | $\text{CN}^-$ | $\text{F}^-$ | $\text{H}_2\text{PO}_4^-$ | $\text{BzO}^-$ | $\text{CH}_3\text{COO}^-$ |
|-----------------------|-----------|---------------|--------------|---------------------------|----------------|---------------------------|
| LOD ( $\mu\text{M}$ ) | <b>3a</b> | 0.58          | 1.35         | 3.03                      | 3.13           | 1.20                      |
|                       | <b>3b</b> | 0.35          | 1.21         | 2.27                      | 3.22           | 0.90                      |
| LOQ ( $\mu\text{M}$ ) | <b>3a</b> | 1.92          | 4.45         | 9.99                      | 10.33          | 3.96                      |
|                       | <b>3b</b> | 1.17          | 3.99         | 7.48                      | 10.63          | 2.97                      |

The tested hydrazones show a remarkable sensitivity to  $\text{CN}^-$ , with a LOD of 0.35  $\mu\text{M}$  (0.035 equiv.) for compound **3b** and 0.58  $\mu\text{M}$  (0.058 equiv.) for compound **3a**. These values are very promising, since we placed the two probes at the highest sensitivity for colorimetric probes for this anion, according to the literature [11–15,30–33]. The two compounds also show an LOD around 1  $\mu\text{M}$  for  $\text{F}^-$  and  $\text{CH}_3\text{COO}^-$ .  $\text{H}_2\text{PO}_4^-$  and  $\text{BzO}^-$  show higher detection limits, between 2.27 and 3.22  $\mu\text{M}$ , for the two compounds.  $\text{BzO}^-$  is the only anion to which compound **3a** is more sensitive than **3b**, although the LOD is still higher when compared to the other anions.

These results indicate that the anion sensing ability of hydrazones **3a–b** may be related to the basicity of each anion, which would cause deprotonation of the NH group [32].

CN<sup>-</sup> is by far the anion in this group with the highest  $K_b$ , and the sensitivity to this anion is significantly higher. Cyanide has the ability to form a very weak acid with H<sup>+</sup> (HCN, pK<sub>a</sub> = 9.1 in water) [32], and is believed to cause deprotonation of this type of compound. This is also correlated with the fact that the anions that do not show an optical change (NO<sub>3</sub><sup>-</sup>, ClO<sub>4</sub><sup>-</sup>, HSO<sub>4</sub><sup>-</sup>, Br<sup>-</sup>, and I<sup>-</sup>) are the ones with a pK<sub>a</sub> lower than 1. On the other hand, F<sup>-</sup> (pK<sub>a</sub> = 3.14), CH<sub>3</sub>COO<sup>-</sup> (pK<sub>a</sub> = 4.75), H<sub>2</sub>PO<sub>4</sub><sup>-</sup> (pK<sub>a</sub> = 7.21), and BzO<sup>-</sup> (pK<sub>a</sub> = 4.19) show significantly higher pK<sub>a</sub> values and show colorimetric changes in the presence of hydrazone **3a–b**, which correlates to the hypothesis of optical changes based on deprotonation of the NH group.

### 3.4. NMR Titrations

The sensitivity of **3b** for CN<sup>-</sup> and F<sup>-</sup>, as observed with the spectrophotometric titrations, was complemented by performing <sup>1</sup>H NMR titrations, to study the binding mode between the hydrazone and the anions and investigate whether deprotonation of the molecule occur. Due to the limited solubility of **3b** in deuterated ACN, the study was carried out in DMSO-*d*<sub>6</sub>.

Figure 7 shows the spectra for the NMR titration of compound **3b** with CN<sup>-</sup>. The compound's original spectrum shows NH at 11.76 ppm and OH at 9.89 ppm. It can be observed that 0.025 equiv. of CN<sup>-</sup> can induce a partial deprotonation of the two groups, due to the basicity of the ion. The imine N=CH and the protons from the dinitrophenyl group (H3, H5, and H6) move to lower chemical shift, due to the shielding effect caused by the deprotonation. The increased electron density, delocalized through the conjugated system, causing the shielding effect, is potentiated by the electron acceptor character of the nitro groups. With the addition of higher amounts of CN<sup>-</sup>, this change becomes clearer: with 0.1 equiv. of CN<sup>-</sup>, NH and OH totally disappear, and the upfield shift of the other signals is significant. Quinoline protons H3', H4', H5', H6', and H7' signals remain similar to the original spectrum.

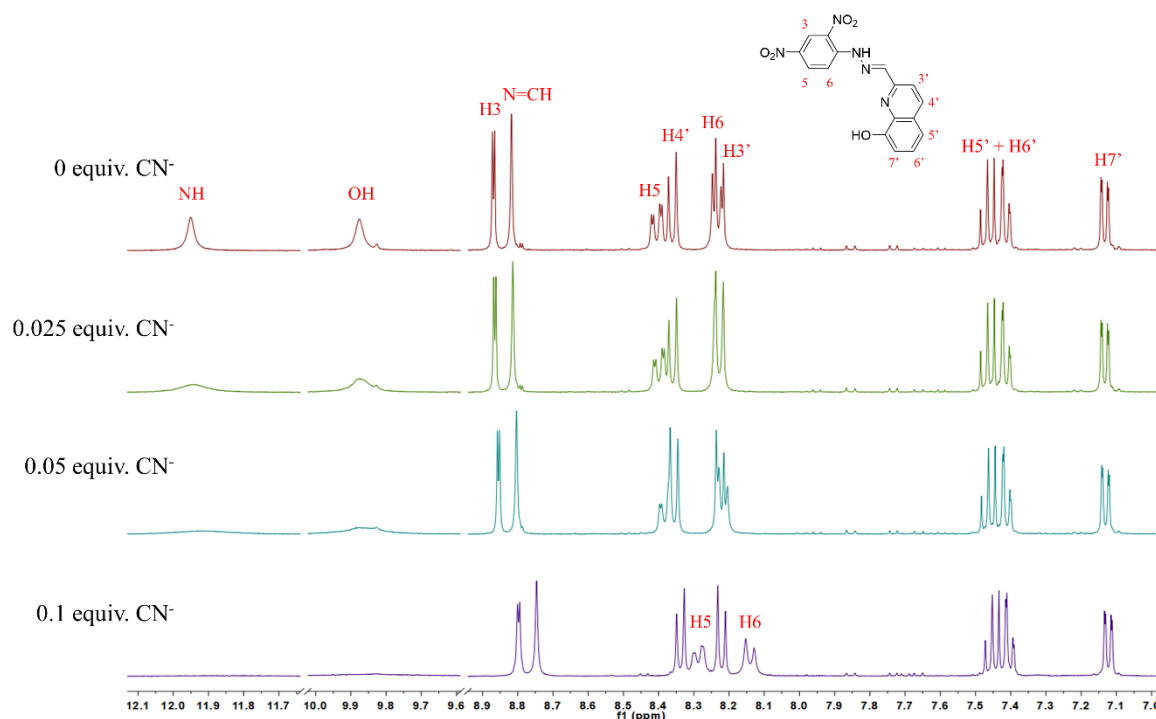
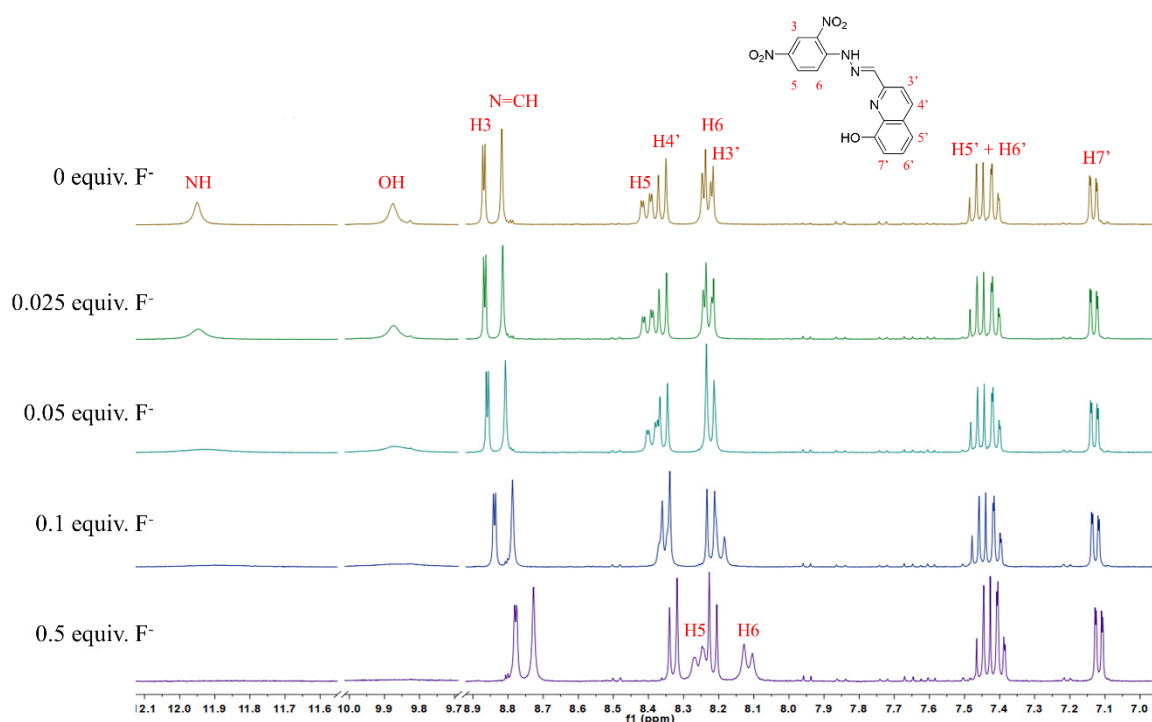


Figure 7. NMR titration of compound **3b** with CN<sup>-</sup> in DMSO-*d*<sub>6</sub>.

Figure 8 shows the spectra for the NMR titration of compound **3b** with F<sup>-</sup>. The interaction is very similar to the interaction with CN<sup>-</sup>, although the sensitivity is lower. This is in accordance with the lower basicity of fluoride. A total of 0.5 equiv. of F<sup>-</sup> are



needed to achieve a similar effect to the one caused by 0.1 equiv. of  $\text{CN}^-$ . Similar upfield shifts occurred for the imine  $\text{N}=\text{CH}$  and  $\text{H}_3$ ,  $\text{H}_5$ , and  $\text{H}_6$ , and quinoline protons  $\text{H}_3'$ ,  $\text{H}_4'$ ,  $\text{H}_5'$ ,  $\text{H}_6'$ , and  $\text{H}_7'$  also remained similar to the original spectrum.



**Figure 8.** NMR titration of compound **3b** with  $\text{F}^-$  in  $\text{DMSO-}d_6$ .

#### 4. Conclusions

This work reports the synthesis and characterization of two novel quinoline-based dinitrophenyl hydrazones, **3a–b**. The two compounds were shown to be sensitive to different anions, namely,  $\text{H}_2\text{PO}_4^-$ ,  $\text{CH}_3\text{COO}^-$ ,  $\text{BzO}^-$ ,  $\text{CN}^-$ , and  $\text{F}^-$ , and the interaction in ACN solutions was tested by spectrophotometric titrations. The stoichiometry of the interactions was assessed by the method of continuous variation. Compound **3b** showed a remarkable sensitivity to  $\text{CN}^-$ , with a LOD of  $0.35 \mu\text{M}$ . This value is below the EU limit, both for drinking and mineral water ( $50$  and  $70 \mu\text{g L}^{-1}$ , respectively, equaling to  $1.92$  and  $2.69 \mu\text{M}$ ). The two compounds are also sensitive for the other anions (LODs in the range of  $\mu\text{M}$ ), based on its basicity.  $^1\text{H}$  NMR titrations were performed to assess the binding site of the molecules, for the interaction between **3b** and  $\text{CN}^-$  and  $\text{F}^-$ , which showed that increasing concentrations of the anion induce deprotonation of both  $\text{NH}$  and  $\text{OH}$ . Sensitivity is higher for  $\text{CN}^-$ , the most basic anion of the group of tested anions.

**Author Contributions:** Conceptualization: M.M.M.R. and S.P.G.C.; formal analysis: R.P.C.L.S., S.P.G.C. and M.M.M.R.; funding acquisition: S.P.G.C., R.B.F. and M.M.M.R.; methodology: S.P.G.C. and M.M.M.R.; investigation: R.P.C.L.S.; writing—original draft preparation: R.P.C.L.S., S.P.G.C. and M.M.M.R.; writing—review and editing: R.P.C.L.S., S.P.G.C., R.B.F. and M.M.M.R.; project administration: S.P.G.C., R.B.F. and M.M.M.R.; resources: S.P.G.C., R.B.F. and M.M.M.R.; supervision: S.P.G.C., R.B.F. and M.M.M.R. All authors have read and agreed to the published version of the manuscript.

**Funding:** Thanks are due to Fundação para a Ciência e Tecnologia (FCT) and FEDER (European Fund for Regional Development)-COMPETE-QRENEU for financial support through the Chemistry Research Centre of the University of Minho (Ref. CQ/UM (UID/QUI/00686/2020)), and a PhD grant to R.P.C.L.S. (SFRH/BD/145639/2019). The NMR spectrometer Bruker Avance III 400 is part of the National NMR Network (PTNMR) and was financially partially supported by Infrastructure Project No. 022161 (co-financed by FEDER through COMPETE 2020, POCI and PORL, and FCT through PIDDAC).

**Institutional Review Board Statement:** Not applicable.

**Informed Consent Statement:** Not applicable.

**Data Availability Statement:** Not applicable.

**Conflicts of Interest:** The authors declare no conflict of interest.

## References

1. Blake, A.; Mclean, V. A Calorimetric Consumption Assay for the Measurement by Cultured Cells of D-Glucose. *Anal. Biochem.* **1989**, *177*, 156–160. [[CrossRef](#)]
2. Chang, C.C.; Chen, C.Y.; Chen, C.P.; Lin, C.W. Facile colorimetric detection of human chorionic gonadotropin based on the peptide-induced aggregation of gold nanoparticles. *Anal. Methods* **2015**, *7*, 29–33. [[CrossRef](#)]
3. Kaur, B.; Kaur, N.; Kumar, S. Colorimetric metal ion sensors—A comprehensive review of the years 2011–2016. *Coord. Chem. Rev.* **2018**, *358*, 13–69. [[CrossRef](#)]
4. Wang, B.; Anslyn, E. Colorimetric sensor design. In *Chemosensors: Principles, Strategies, and Applications*; Wiley: Hoboken, NJ, USA, 2011; pp. 275–295.
5. Berhanu, A.L.; Gaurav; Mohiuddin, I.; Malik, A.K.; Aulakh, J.S.; Kumar, V.; Kim, K.H. A review of the applications of Schiff bases as optical chemical sensors. *TrAC—Trends Anal. Chem.* **2019**, *116*, 74–91. [[CrossRef](#)]
6. McDonagh, C.; Burke, C.S.; MacCraith, B.D. Optical chemical sensors. *Chem. Rev.* **2008**, *108*, 400–422. [[CrossRef](#)]
7. Sousa, R.P.C.L.; Figueira, R.B.; Costa, S.P.G.; Raposo, M.M. Optical fiber sensors for biocide monitoring: Examples, transduction materials, and prospects. *ACS Sens.* **2020**, *5*, 3678–3709. [[CrossRef](#)]
8. Junaid, H.M.; Batool, M.; Harun, F.W.; Akhter, M.S.; Shabbir, N. Naked Eye Chemosensing of Anions by Schiff Bases. *Crit. Rev. Anal. Chem.* **2020**, *52*, 463–480. [[CrossRef](#)]
9. Gale, P.A.; Caltagirone, C. Fluorescent and colorimetric sensors for anionic species. *Coord. Chem. Rev.* **2018**, *354*, 2–27. [[CrossRef](#)]
10. Jali, B.R.; Barick, A.K.; Mohapatra, P.; Sahoo, S.K. A comprehensive review on quinones based fluoride selective colorimetric and fluorescence chemosensors. *J. Fluor. Chem.* **2021**, *244*, 109744. [[CrossRef](#)]
11. Udhayakumari, D. Chromogenic and fluorogenic chemosensors for lethal cyanide ion. A comprehensive review of the year 2016. *Sens. Actuators B Chem.* **2018**, *259*, 1022–1057. [[CrossRef](#)]
12. Wang, F.; Wang, L.; Chen, X.; Yoon, J. Recent progress in the development of fluorometric and colorimetric chemosensors for detection of cyanide ions. *Chem. Soc. Rev.* **2014**, *43*, 4312–4324. [[CrossRef](#)] [[PubMed](#)]
13. Xu, Z.; Chen, X.; Kim, H.N.; Yoon, J. Sensors for the optical detection of cyanide ion. *Chem. Soc. Rev.* **2009**, *39*, 127–137. [[CrossRef](#)] [[PubMed](#)]
14. Ma, J.; Dasgupta, P.K. Recent developments in cyanide detection: A review. *Anal. Chim. Acta* **2010**, *673*, 117–125. [[CrossRef](#)] [[PubMed](#)]
15. Aldrey, A.; Núñez, C.; García, V.; Bastida, R.; Lodeiro, C.; Macías, A. Anion sensing properties of new colorimetric chemosensors based on macrocyclic ligands bearing three nitrophenylurea groups. *Tetrahedron* **2010**, *66*, 9223–9230. [[CrossRef](#)]
16. Pal, A.; Karmakar, M.; Bhatta, S.R.; Thakur, A. A detailed insight into anion sensing based on intramolecular charge transfer (ICT) mechanism: A comprehensive review of the years 2016 to 2021. *Coord. Chem. Rev.* **2021**, *448*, 214167. [[CrossRef](#)]
17. Tay, H.M.; Beer, P. Optical sensing of anions by macrocyclic and interlocked hosts. *Org. Biomol. Chem.* **2021**, *19*, 4652–4677. [[CrossRef](#)]
18. McNaughton, D.A.; Fares, M.; Picci, G.; Gale, P.A.; Caltagirone, C. Advances in fluorescent and colorimetric sensors for anionic species. *Coord. Chem. Rev.* **2021**, *427*, 213573. [[CrossRef](#)]
19. Jali, B.R.; Baruah, J.B. Recent progress in Schiff bases in detections of fluoride ions. *Dyes Pigm.* **2021**, *194*, 109575. [[CrossRef](#)]
20. El-Sherif, A.A.; Aljahdali, M.S. Review: Protonation, complex-formation equilibria, and metal–ligand interaction of salicylaldehyde Schiff bases. *J. Coord. Chem.* **2013**, *66*, 3423–3468. [[CrossRef](#)]
21. Jabeen, M. A comprehensive review on analytical applications of hydrazone derivatives. *J. Turk. Chem. Soc. Sect. A Chem.* **2022**, *9*, 663–698. [[CrossRef](#)]
22. Yang, Y.; Gao, C.Y.; Liu, J.; Dong, D. Recent developments in rhodamine salicylidene hydrazone chemosensors. *Anal. Methods* **2016**, *8*, 2863–2871. [[CrossRef](#)]
23. Khattab, T.A.; Gaffer, H.E. Synthesis and application of novel tricyanofuran hydrazone dyes as sensors for detection of microbes. *Color. Technol.* **2016**, *132*, 460–465. [[CrossRef](#)]
24. Farshbaf, S.; Anzenbacher, P. Fluorimetric sensing of ATP in water by an imidazolium hydrazone based sensor. *Chem. Commun.* **2019**, *55*, 1770–1773. [[CrossRef](#)]
25. Wu, W.N.; Wu, H.; Wang, Y.; Mao, X.J.; Liu, B.Z.; Zhao, X.L.; Xu, Z.Q.; Fan, Y.C.; Xu, Z.H. A simple hydrazone as a multianalyte ( $\text{Cu}^{2+}$ ,  $\text{Al}^{3+}$ ,  $\text{Zn}^{2+}$ ) sensor at different pH values and the resultant  $\text{Al}^{3+}$  complex as a sensor for  $\text{F}^-$ . *RSC Adv.* **2018**, *8*, 5640–5646. [[CrossRef](#)] [[PubMed](#)]
26. Chen, W.; Liang, H.; Wen, X.; Li, Z.; Xiong, H.; Tian, Q.; Yan, M.; Tan, Y.; Royal, G. Synchronous colorimetric determination of  $\text{CN}^-$ ,  $\text{F}^-$ , and  $\text{H}_2\text{PO}_4^-$  based on structural manipulation of hydrazone sensors. *Inorg. Chim. Acta* **2022**, *532*, 120760. [[CrossRef](#)]

27. Xu, H.; Wang, X.; Zhang, C.; Wu, Y.; Liu, Z. Coumarin-hydrazone based high selective fluorescence sensor for copper(II) detection in aqueous solution. *Inorg. Chem. Commun.* **2013**, *34*, 8–11. [[CrossRef](#)]
28. Su, X.; Aprahamian, I. Hydrazone-based switches, metallo-assemblies and sensors. *Chem. Soc. Rev.* **2014**, *43*, 1963–1981. [[CrossRef](#)]
29. Thomsen, V.; Schatzlein, D.; Mercurio, D. Limits of detection in spectroscopy. *Spectroscopy* **2003**, *18*, 103.
30. Batista, R.M.F.; Costa, S.P.G.; Raposo, M.M.M. Naphthyl-imidazo-anthraquinones as novel colorimetric and fluorimetric chemosensors for ion sensing. *J. Photochem. Photobiol. A Chem.* **2013**, *259*, 33–40. [[CrossRef](#)]
31. Batista, R.M.F.; Costa, S.P.G.; Raposo, M.M.M. Selective colorimetric and fluorimetric detection of cyanide in aqueous solution using novel heterocyclic imidazo-anthraquinones. *Sens. Actuators B Chem.* **2014**, *191*, 791–799. [[CrossRef](#)]
32. Cao, J.; Wang, X.M. An investigation of the deprotonation of hydrazone-based receptors on interaction with anion: Develop a colorimetric system distinguishing cyanide from anions. *Tetrahedron* **2013**, *69*, 10267–10271. [[CrossRef](#)]
33. Batista, R.M.F.; Oliveira, E.; Costa, S.P.G.; Lodeiro, C.; Raposo, M.M.M. Cyanide and fluoride colorimetric sensing by novel imidazo-anthraquinones functionalised with indole and carbazole. *Supramol. Chem.* **2014**, *26*, 71–80. [[CrossRef](#)]